# Disconnected Glass-Glass Transitions and Diffusion Anomalies in a Model with Two Repulsive Length Scales

Matthias Sperl

*Institut für Materialphysik im Weltraum, Deutsches Zentrum für Luft- und Raumfahrt, 51170 Köln, Germany*

Emanuela Zaccarelli and Francesco Sciortino

*Dipartimento di Fisica and CNR-ISC, Universitá di Roma La Sapienza, Piazzale A. Moro 2, 00185 Roma, Italy*

Pradeep Kumar

*Center for Studies in Physics and Biology, Rockefeller University, New York, New York 10021, USA*

H. Eugene Stanley

*Department of Physics and Center for Polymer Studies, Boston University, Boston, Massachusetts 02215, USA*

Building on mode-coupling-theory calculations, we report a novel scenario for multiple glass transitions in a purely repulsive spherical potential: the square shoulder. The liquid-glass transition lines exhibit both melting by cooling and melting by compression as well as associated diffusion anomalies, similar to the ones observed in water. Differently from all previously investigated models, we find for small shoulder widths a glass-glass line that is disconnected from the liquid phase. Upon increasing the shoulder width such a glass-glass line merges with the liquid-glass transition lines, featuring two distinct end point singularities that give rise to logarithmic decays in the dynamics. We analytically explain these findings by considering the interplay of different repulsive length scales.

In the field of glassy slow dynamics, many experiments and simulations have been inspired in recent years by the mode-coupling theory (MCT) of the glass transition [1]. The theory deals with density autocorrelation functions $\phi_q(t)$ with wave vectors $q$, and predicts their long-time limits $f_q$. While in the liquid state $f_q = 0$, the glass state is defined by $f_q > 0$. MCT was first applied to the hard-sphere system (HSS) where a liquid-glass transition was identified [2], and confirmed by experiments [3]. In addition to liquid-glass transitions, for certain interactions MCT also predicts glass-glass transitions: In this case an existing first glass state with $f_q^1$ transforms into a second distinct glass state with $f_q^2 > f_q^1$ discontinuously. Such glass-glass transitions were predicted for the square-well system (SWS) where the hard-core repulsion is supplemented by a short-ranged attraction [4–6]. In the SWS, the first glass state is driven by repulsion like in the HSS and the second glass state is driven by attraction. The competition between these two mechanisms is responsible for the emergence of glass-glass transitions. Such a line of glass-glass transitions extends smoothly a line of liquid-glass transitions into the glass state and terminates in an end point singularity. Close to the end point singularity the dynamics is ruled by logarithmic relaxation [7]. The predicted logarithmic decays were identified in computer simulations and establish the relevance of end point singularities for the description of glassy dynamics [8,9]. A second dynamical anomaly predicted for the SWS concerns a reentrant liquid-glass line that causes melting by

cooling [4–6]. This prediction of MCT was confirmed by computer simulation [10] and by experiments in colloidal suspensions [11,12]. For a comparison of the MCT results with experiments a clarification seems appropriate: All glass and glass-glass transitions cited above or presented in the following refer to the kinetic glass transition at $T_c$ or $\phi_c$ and not to a thermodynamic transition. For molecular systems, the relaxation time exhibits a large increase already around $T_c$ but does not actually diverge within the usually very large available experimental windows.

In this work we replace the attractive length scale in the SWS by a second repulsive length scale $\delta$ of the square-shoulder system (SSS) as shown in Fig. 1. The particle diameter $d$ is set to unity in the following. The SSS can be considered the simplest potential with two competing interparticle distances; it is applied to describe properties of
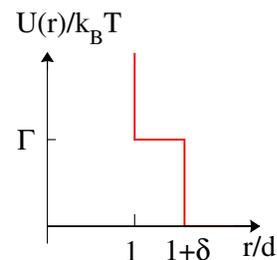


FIG. 1 (color online).　Square-shoulder potential with control parameters packing fraction $\varphi = \pi\rho d^3/6$, shoulder height $\Gamma = u_0/k_B T$, and shoulder width $\delta$ for particles of diameter $d$ at density $\rho$.

metallic glasses like cerium or cesium [13], micellar [14] and granular materials [15], silica [16], and water [17].

In the following, the glass-transition diagrams are calculated from the singularities in the roots of the MCT functional [1]

$$\mathcal{F}_q[\mathbf{V}, f_k] = \sum_{\vec{k}+\vec{p}=\vec{q}} V_{q,kp} f_k f_p = \frac{f_q}{1 - f_q}, \quad (1a)$$

with vertex **V** given by wave vector moduli $q$, $k$, $p$, the static structure factor $S_q$, and the direct correlation function $c_q$:

$$V_{q,kp} = \rho S_q S_k S_p \{\vec{q} \cdot [\vec{k} c_k + \vec{p} c_p]\}^2 / q^4. \quad (1b)$$

Quantities $S_q$ and $c_q$ are given by the interaction potential. The discretization of the functionals is chosen as for the HSS and the SWS [5,18] with a number of wave vectors $M = 600$ and a wave vector cutoff $dq_{max} = 80$, and the static structure factors of the SSS are obtained within the Rogers-Young approximation [19,20]. Further details of the calculations shall be found in a subsequent publication [21]. For specific values of the control parameters packing fraction $\varphi$, shoulder height $\Gamma$, and shoulder width $\delta$, Eq. (1) exhibits singularities where the $f_q$ change discontinuously indicating liquid-glass or glass-glass transitions. At these singularities one can define the so-called exponent parameter $\lambda < 1$ that fixes all other critical exponents of the theory [1]. While typically at liquid-glass transitions, $\lambda \approx 0.7$, $\lambda$ approaches unity at the end point of glass-glass transition lines signaling the emergence of logarithmic decay laws [7].

Figure 2(a) shows the glass-transition scenario for $\delta = 0.13$: The liquid-glass transition line (diamonds) starts at the HSS limiting value of $\varphi_{HSS}^c = 0.5206$ (dashed line for small $\Gamma$) for vanishing shoulder width $\Gamma$. For increasing shoulders and up to $\Gamma \approx 1.5$, the curve exhibits a shift in the transition packing fraction $\varphi(\Gamma)$ to higher values—the glass initially melts upon cooling. This trend can be traced to the evolution of the static structure factor which becomes sharper and moves to lower wave vectors for higher $\Gamma$; the corresponding pair distribution functions show a higher probability for particles being at larger distances from each other. Hence, larger particle separations weaken the cage and are compensated by higher densities at the glass transition. For states above the glass transition this means that the relaxation in the system may initially speed up when increasing the shoulder. For shoulder heights from $2k_BT$ to $3.5k_BT$, i.e., for $2 \lesssim \Gamma \lesssim 3.5$, the glass-transition curve bends downwards and reaches the limiting value of the HSS for the outer core $\hat{\varphi}_{HSS}^c = \varphi_{HSS}^c/(1 + \delta)^3 = 0.3608$ (dashed line for large $\Gamma$).

If the packing fractions and repulsive strengths are increased beyond the liquid-glass transition line, one encounters an additional line of glass-glass-transition singularities (filled circles). Differently from glass-glass lines in all models investigated previously, this additional line is lo-
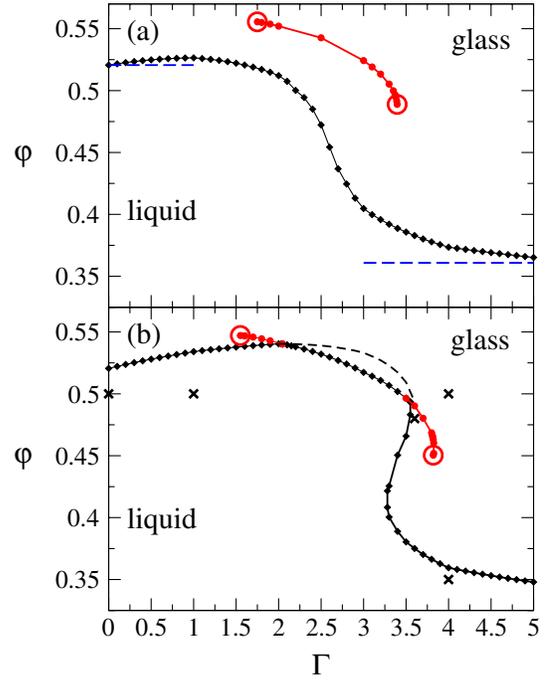


FIG. 2 (color online).   Glass-transition diagrams for the SSS. Diamonds ($\blacklozenge$) indicate liquid-glass transitions, filled circles ($\bullet$) show glass-glass transition points terminating in two end point singularities ($\bigcirc$). (a) $\delta = 0.13$. Dashed lines display the respective limits for hard spheres of diameter 1 and $1 + \delta$. The line of glass-glass transitions is disconnected from the line of liquid-glass transitions, and moves towards and crosses it for larger shoulder width. (b) $\delta = 0.15$. Crosses ($\times$) indicate the five states discussed in Fig. 3 relating the glass-glass transitions to features in the static structure. The dashed curve exhibits the liquid-glass transition line for a reduced wave vector cutoff of $dq_{max} = 40$ demonstrating that without contributions of higher wave vectors to the functional in Eq. (1) the lines of glass-glass transitions are absent.

cated inside the glassy regime, disconnected from any liquid-glass transition line. It is bounded by two end point singularities (open circles) where the additional discontinuity in the $f_q$ vanishes.

When increasing the shoulder width further, the glass-glass and liquid-glass transition lines move towards each other and start to merge for sufficiently high shoulders at around $\delta = 0.145$. Figure 2(b) shows the situation for $\delta = 0.15$: From $\Gamma = 2.0$ to 3.5, the former glass-glass line now indicates a transition from the liquid directly into the second glass state. For $\Gamma < 2.0$ and for $\Gamma > 3.5$, the formerly isolated glass-glass line crosses the liquid-glass line and extends into the glassy regime as two glass-glass transition lines.

Figure 2(b) also exhibits the reentry phenomenon melting by cooling for small $\Gamma$ as discussed before for $\delta = 0.13$, but in addition a second reentry phenomenon is found between $\Gamma = 3.0$ and 3.5, where melting can also be induced by compression. The trends can again be traced back to the behavior of the static structure: Increasing the pack-

ing fraction from low values to around $\varphi \approx 0.45$, the pair distribution function shows an increased probability for particle contact at both inner and outer cores. However, for values larger than $\varphi \approx 0.45$, the contact at the inner core grows at the expense of contact at the outer core; interparticle contacts at the outer core are suppressed by the high density and particles now collide much more frequently at their inner cores. Since the cage represented by the inner core is too loose to trigger glassy arrest at such density, this is compensated by lower temperature (or equivalently by higher $\Gamma$) at the glass transition.

For the explanation of the glass-glass transitions, it is necessary to identify contributions to the functionals in Eq. (1) that come from wave vectors other than the principal peaks of $S_q$. It will be shown that for the SSS, the interplay between the hard and the soft core introduces changes in the contact values of the pair distribution function that are responsible for the glass-glass transitions. Figure 3 shows $g(r)$ for the five states indicated in Fig. 2(b). Strong repulsion at a specific interparticle distance leads to an increase in the contact value of $g(r)$ [22]. While $g(r)$ for the HSS only exhibits a contact value at $r/d = 1$ (cf. filled circle in Fig. 3), for finite shoulder a second contact value emerges at $r/d = 1 + \delta$ (cf. squares in Fig. 3). If the outer core becomes dominant, the contact value at the inner core becomes suppressed (cf. triangles in Fig. 3), and for intermediate states, both contact values can become equally important (cf. diamonds in Fig. 3). Stars in Fig. 3 for an intermediate point between the glass and the glass-glass transition show that the structural trend continues smoothly across the glass-glass transition. It is known from the theory of Fourier transformations that the discontinuities of $g(r)$, e.g., the contact values, determine the
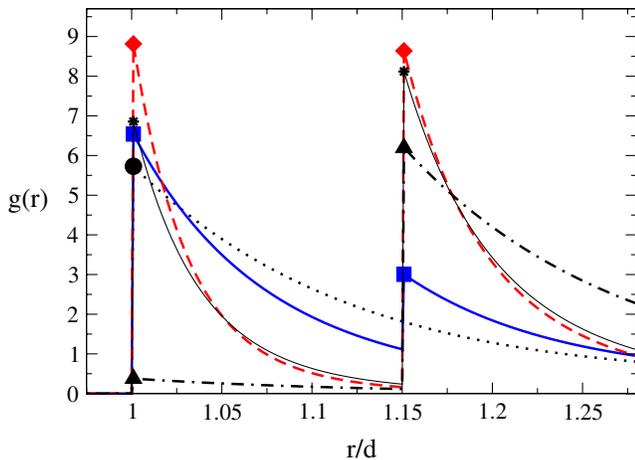


FIG. 3 (color online). Pair distribution functions $g(r)$ and contact values as filled symbols for the five states indicated by crosses in Fig. 2(b): $(\Gamma, \varphi) = (0.0, 0.5)$, circle; (1.0, 0.5), squares; (4.0, 0.5), diamonds; (4.0, 0.35), triangles; (3.6, 0.48), stars. Higher contact values $B(\varphi)$ generate additional contributions to the functional in Eq. (1) and can allow for glass-glass transition lines as in Figs. 2(a) and 2(b) if the contributions are large enough. See text for discussion.

large wave vector behavior of $S_q$ and $c_q$ [23]. $S_q$ and $c_q$ in turn enter in the MCT through Eq. (1b).

For a qualitative picture, it is enough to assume two hard-core repulsions at $r/d = 1$ and $r/d = 1 + \delta$ in Percus-Yevick (PY) approximation. For PY, the contact value is known analytically [24], $B(\varphi) = (1 + \varphi/2)/(1 - \varphi)^2$. Hence, for large enough wave vectors, $c_q$ for a single core becomes $c_q^{\text{asy}} = B(\varphi)\cos(q)/q^2$. Inner and outer core have the respective contributions $c_1^{\text{asy}}(q) = B_1 \cos(q)/q^2$ and $c_2(q) = B_2 \cos(q[1 + \delta])/q^2$, where factors of $(1 + \delta)$ in $q^2$ were absorbed into $B_2$. The interference of the two oscillations of different frequency, $c_1^{\text{asy}}(q) + c_2^{\text{asy}}(q)$, results in a beating with an amplitude, that can become twice as large as the individual oscillations, and an interference frequency $d\Delta q = 2\pi/\delta$, e.g., for $\delta = 0.15$ one gets $\Delta q \approx 42d^{-1}$. As a consequence, the interference of the two contact values seen in Fig. 3 creates additional contributions in Eq. (1b) from the tail in $c_q$ between $qd = 20$ and 80, and these additional contributions allow for the possibility of a glass-glass transition as seen in Fig. 2.

To show explicitly that the large-$q$ contributions cause the glass-glass transition line, we eliminate these contributions from the functional by shifting the wave vector cutoff from $qd = 80$ to $qd = 40$ and perform additional calculations. The result is shown in Fig. 2(b) as the dashed line. With the beating now switched off, the dashed line of liquid-glass transitions is recovered without any indication of crossings or glass-glass transitions. For other potentials with sufficiently distinct length scales, e.g., a linear ramp instead of a square shoulder, similar arguments hold. Hence, the glass-glass transitions can also occur for somewhat smoother potentials.

In summary, the following physical picture of the glass-glass transitions emerges: Upon crossing the glass-glass transition line, the localization mechanism of the glass changes from the inner to the outer shell. The localization length decreases drastically since the free space between outer and inner core is no longer available to the particles. At the upper end point, the system is so dense and the shoulder so low that it is no longer possible to arrest at the outer shell, the arrest always takes place at the inner shell, and hence the glass-glass transition vanishes. At the lower end point, the density is too low to force a transition from the outer to the inner shell, and the glass-glass transition vanishes as well.

To make contact with experimental systems, we redraw the transition diagram of Fig. 2(b) in a pressure versus temperature, $P$-$T$, diagram in Fig. 4, using the Rogers-Young thermodynamically consistent equation of state. For a path of constant $T$ and variable $P$, the diffusivity of the dynamics varies with the distance from the liquid-glass transition line. For example, for $T \approx 0.35u_0/k_B$ and starting from low $P$, the diffusivity first decreases until $P \approx 15u_0/d^3$, then it increases anomalously until around $P \approx 30u_0/d^3$, and then it decreases again. Such behavior, known as diffusion anomaly, is experimentally observed
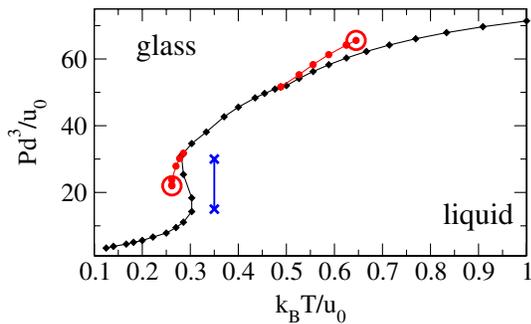
FIG. 4 (color online).　Data from Fig. 2(b) for $\delta = 0.15$ shown with variables pressure $P$ and temperature $T$. Crosses ($\times$) delimit the approximate region for a diffusion anomaly. Above and below that region, the diffusion coefficient decreases with pressure; within the region the diffusion coefficient increases with pressure $P$.

in liquid water [25]. Changing pressure and temperature while measuring the diffusion in the fluid regime is possible in experiments; the remaining parameters $d$ and $u_0$ were estimated recently for models of water [26].

In conclusion, MCT calculations predict for the square-shoulder system three novel features in the glass-transition diagram: (1) melting by cooling, (2) melting by compression—both induced by a disruption of the local structure—and (3) a glass-glass transition line with two end points which is caused by a discontinuous transition between localization at the inner and the outer core of the particles. For comparison with experiments and computer simulation studies, a few additional (partly well-known) findings need to be considered. First, since both MCT and the theory for $S_q$ involve approximations, shifts in the numerical values for the transition points are expected, i.e., the transition for hard spheres is found for $\varphi \approx 0.58$, which is 10% higher than calculated. However, the qualitative predictions for the reentry and glass-glass transitions were found remarkably robust [11,12]. Second, for measurements over large enough windows in time, also activated processes become relevant for the relaxation that are not captured by the idealized theory [1]. Earlier work suggests that those processes come into play late enough to allow for sufficient windows in time to test the theory [3,12]. Third, the relevance of the glass-glass transition scenario found here goes beyond the specific square-shoulder potential: The competition between two repulsive length scales and the presence of diffusion anomalies are observed in several different contexts, ranging from soft matter systems [14,27] to silica [16] and complex liquids [26,28,29]. Our work opens a perspective for understanding slow dynamics in these disparate systems.

[1] W. Götze, *Complex Dynamics of Glass-Forming Liquids: A Mode-Coupling Theory* (Oxford University Press, Oxford, 2009).
[2] U. Bengtzelius, W. Götze, and A. Sjölander, J. Phys. C **17**, 5915 (1984).
[3] W. van Megen and P. N. Pusey, Phys. Rev. A **43**, 5429 (1991).
[4] J. Bergenholtz and M. Fuchs, Phys. Rev. E **59**, 5706 (1999).
[5] K. Dawson, G. Foffi, M. Fuchs, W. Götze, F. Sciortino, M. Sperl, P. Tartaglia, T. Voigtmann, and E. Zaccarelli, Phys. Rev. E **63**, 011401 (2000).
[6] L. Fabbian, W. Götze, F. Sciortino, P. Tartaglia, and F. Thiery, Phys. Rev. E **59**, R1347 (1999).
[7] W. Götze and M. Sperl, Phys. Rev. E **66**, 011405 (2002).
[8] A. M. Puertas, M. Fuchs, and M. E. Cates, Phys. Rev. E **67**, 031406 (2003).
[9] F. Sciortino, P. Tartaglia, and E. Zaccarelli, Phys. Rev. Lett. **91**, 268301 (2003).
[10] G. Foffi, K. A. Dawson, S. V. Buldyrev, F. Sciortino, E. Zaccarelli, and P. Tartaglia, Phys. Rev. E **65**, 050802 (2002).
[11] T. Eckert and E. Bartsch, Phys. Rev. Lett. **89**, 125701 (2002).
[12] K. N. Pham, S. U. Egelhaaf, P. N. Pusey, and W. C. K. Poon, Phys. Rev. E **69**, 011503 (2004).
[13] D. A. Young and B. J. Alder, Phys. Rev. Lett. **38**, 1213 (1977).
[14] N. Osterman, D. Babic, I. Poberaj, J. Dobnikar, and P. Ziherl, Phys. Rev. Lett. **99**, 248301 (2007).
[15] J. Duran, *Sands, Powders, and Grains: An Introduction to the Physics of Granular Materials* (Springer, New York, 1999).
[16] J. Horbach, J. Phys. Condens. Matter **20**, 244118 (2008).
[17] E. A. Jagla, J. Chem. Phys. **111**, 8980 (1999).
[18] T. Franosch, M. Fuchs, W. Götze, M. R. Mayr, and A. P. Singh, Phys. Rev. E **55**, 7153 (1997).
[19] F. J. Rogers and D. A. Young, Phys. Rev. A **30**, 999 (1984).
[20] A. Lang, G. Kahl, C. N. Likos, H. Löwen, and M. Watzlawek, J. Phys. Condens. Matter **11**, 10 143 (1999).
[21] M. Sperl, E. Zaccarelli, F. Sciortino, P. Kumar, and H. E. Stanley (to be published).
[22] J.-P. Hansen and I. R. McDonald, *Theory of Simple Liquids* (Academic, London, 1986), 2nd ed.
[23] M. J. Lighthill, *Introduction to Fourier Analysis and Generalized Functions* (Cambridge University Press, Cambridge, England, 1962).
[24] M. S. Wertheim, Phys. Rev. Lett. **10**, 321 (1963).
[25] C. A. Angell, E. D. Finch, and P. Bach, J. Chem. Phys. **65**, 3063 (1976).
[26] Z. Yan, S. V. Buldyrev, P. Kumar, N. Giovambattista, and H. E. Stanley, Phys. Rev. E **77**, 042201 (2008).
[27] G. Foffi, F. Sciortino, P. Tartaglia, E. Zaccarelli, F. LoVerso, L. Reatto, K. A. Dawson, and C. N. Likos, Phys. Rev. Lett. **90**, 238301 (2003).
[28] N. V. Gribova, Y. D. Fomin, D. Frenkel, and V. N. Ryzhov, Phys. Rev. E **79**, 051202 (2009).
[29] N. N. Barraz, E. Salcedo, and M. C. Barbosa, J. Chem. Phys. **131**, 094504 (2009).